ACS APPLIED MATERIALS & INTERFACES

Research Article

www.acsami.org

Looking over Liquid Silicone Rubbers: (2) Mechanical Properties vs Network Topology

Etienne Delebecq,[†] Nicolas Hermeline,[‡] Alain Flers,[‡] and François Ganachaud*[,†,§,⊥]

[†]Ingénierie des Architectures Macromoléculaires, UMR 5076 CNRS/ENSCM, 8 Rue de l'Ecole Normale, 34296 Montpellier Cedex, France

[‡]FCI ResearchTechnical Center, Rue des Longs Réages, 28231 Epernon, France

[§]Université de Lyon, F-69003, France

[⊥]INSA-Lyon, IMP, UMR5223, F-69621Villeurbanne, France

Supporting Information

ABSTRACT: In the previous paper of this series, eight formulations were analyzed under their uncross-linked forms to relate liquid silicone rubber (LSR) chemical compositions to material network topologies. Such topologies were confirmed by swelling measurements and hardness evaluation on vulcanized samples. In this article, characterization of cross-linked materials is further done using different mechanical measurements on final materials, including dynamic mechanical analysis, compression set, stress−strain behavior and tear resistance. It was shown that the compression set value is mainly related to the chains motion: increasing the filler−polymer interactions and/or decreasing the dangling/untethered chains content positively impact the compression resistance. Elongation at break depends on the molar mass between cross-linking points, showing an optimum value set at around 20 000 g mol^{-1}, i.e., the critical mass between entanglements. The distribution of elastic strands into the network has strong implications on the stress−strain curves profiles. By generating bimodal networks, the ultimate properties are enhanced. The materials cured by hydride addition on vinyl groups catalyzed by peroxide exhibit poorer compression set and tensile strength values, respectively, because of post-cross-linking reaction and broad polydispersity index of elastic network chains.

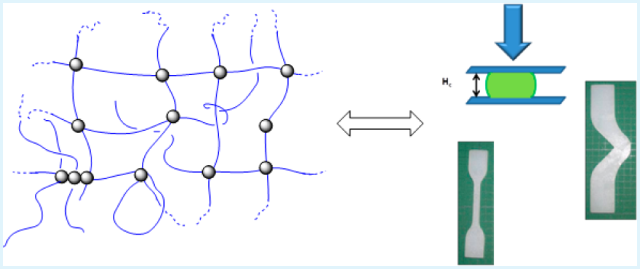

KEYWORDS: *liquid silicone rubber, platinum cured silicones, mechanical properties, compression set, tensile tests, tear resistance*

1. INTRODUCTION

Thanks to their excellent properties such as superior elongation at break, hydrophobicity, wide operating temperature range, and fast cure properties, liquid silicone rubbers lend themselves to a vast spectrum of applications, in particular for sealing and joint applications. In the previous paper of this series,[1] eight commercial formulations used in automotive applications were chemically characterized under their un-cross-linked forms (vide infra) before being cured by injection-molding at 180 and 200 °C. We determined the filler content, the architecture and molar mass of each prepolymers as well as the nature, environment, and concentration of functional groups. Table 1 sums up the main differences observed between formulations as determined from chemical analyses, and Scheme 1 gives a full picture of the chemistry and physical-chemistry involved in these materials.[1]

Liquid silicone rubber (LSR) formulations are mainly composed of long α,ω-divinyl polydimethylsiloxane chains, short SiH-multifunctionalized copolymers, silica, and platinum as a hydrosilylation catalyst. The long chains enable high control on the molar mass between cross-linking points (M_c). To control the hardness of the materials up to 30 Shore A, one simply adjusts the silica content, whereas harder materials are obtained by decreasing the molar mass between cross-linking points. This can be done either by varying the molar mass of the vinyl terminated polymer and/or by incorporating few vinyl groups inside the backbone of the polymer (monomer unit named D^{Vi} according to the GE's nomenclature). In presence of platinum catalyst, poly(methylhydro-*co*-dimethyl)siloxane acts as cross-linker. Depending on the distribution of the functional groups in the cross-linker chain, the ratio between hydride and vinyl groups ranges from 1.6 for well redistributed, up to 3.7 for non redistributed methylhydrosiloxane units in the cross-linker chain (redistribution reaction scrambles dimethylsiloxane and methylhydrosiloxane copolymer units and thus spaces out the functional group SiH in the chain) (Table 1). Strong consequences on the material network structure were found: the hydride groups in excess induce side reactions that form additional short bridges between cross-linker molecules, i.e., highly cross-linked domains (Scheme 1). Note that we have

Received: March 21, 2012
Accepted: July 2, 2012
Published: July 2, 2012

 © 2012 American Chemical Society

Table 1. Main parameters Describing the Chemical Compositions and Network Topologies of LSR formulations as Determined from Chemical Analyses[1]

formulation	hardness[a] (Shore A)	$\frac{SiH}{SiVi}$	catalysis system	silica surface groups	silica content (%)	M_c^{Theo} [b] (kg/mol)
1	29	3.7	platinum	methyl	29	43.3
2	30	1.8	platinum	vinyl	28	41.0
4	31	2.3	platinum	methyl	31	47.3
6	33	1.4	peroxyde + platinum	methyl	28	34.8
7	50	1.6	peroxyde + platinum	vinyl	31	13.1
8	32	2.1	platinum	vinyl	28	16.8

[a]Hardness given by suppliers. [b]M_c^{Theo} corresponds to the expected molar mass between cross-links according to the chemical analysis.

Scheme 1. Main Structures Observed in LSR Formulations and Schematic Representation of a Nonperfect Silicone Polymer Network Formed by End-Linking Reactions

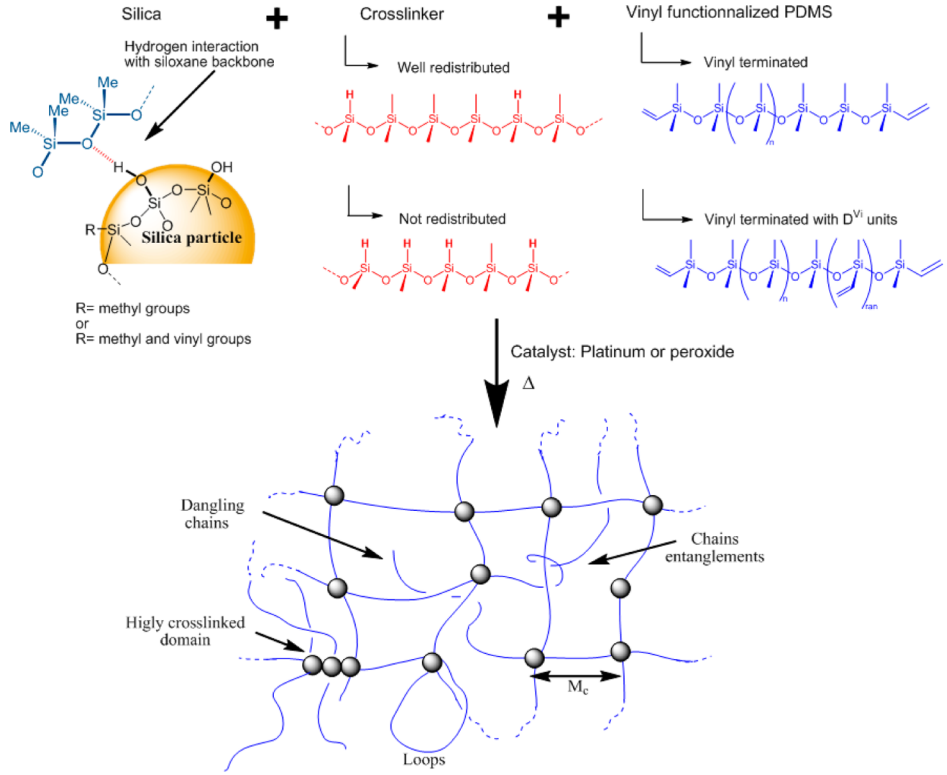

shown that some formulations use a double curing system, combining platinum and peroxide catalysts.From these results, the reactivity and networks topologies of different samples were predicted and confirmed by (i) evaluating the curing behavior; (ii) investigating the final material in terms of molar mass between cross-linking points (M_c) and physical cross-linking between filler surface and PDMS network (expressed as V_r^{Ph}, see Table S1 in the Supporting Information and ref 1 for details). Formulation **1** contains high excess of hydride groups forming extra cross-linking points to generate highly cross-linked domains; formulation **2** entails two cross-linkers of different chain lengths; vinyl-modified silica was found in materials **2** and **7**. Some formulations also include methyl-vinylsiloxane units (D^{Vi}) in the polymer chains, below 0.2 D^{Vi} per chains on average for materials **2** and **6** and up to 1.36 and 0.85 for materials **7** and **8**, respectively. These randomly distributed structures are suspected to cause broadening of the polydispersity index of the elastic network strands. Formulations **6** and **7** are cured through a combination of platinum and peroxide catalysts. Radical reaction would induce reaction of vinyl groups on methyl, creating less controlled network architectures. Finally, formulation **8** is thought to incorporate neutral PDMS chains.

In the following, we first ought to summarize the different molecular physics theories available in the open literature to simulate the behavior of thoroughly controlled silicone network topologies, using model silicone chains and mastered cross-linking chemistries. Contrary to methods and results developed in this section, our approach in this series of papers is different: here, a priori unknown industrial products far from "perfect" networks are chemically characterized and then mechanically analyzed after curing. The commercial formulations that we studied in the previous paper of this series indeed entailed complex topologies, with a variety of molar masses between cross-linking points, contents of defects, and hydrogen bonding densities between polymer and filler. In the present paper, we further investigate these final materials by relating "chemically understood" and "experimental" topologies (M_c, tan δ) and the mechanical properties such as tensile and tear strength and compression set of these materials. In a final discussion, we gather all the tendencies found in chemistry, physical chemistry,

dx.doi.org/10.1021/am300503j | ACS Appl. Mater. Interfaces 2012, 4, 3353−3363

and mechanics of these materials to discuss the influence of network parameters on mechanical properties.

2. LITERATURE SURVEY OF THEORIES ON MECHANICAL PROPERTIES OF MODEL SILICONE ELASTOMERS

2.1. Viscoelasticity versus Network Topology of Unfilled Materials. Polydimethylsiloxane has been used for decades as a polymer of choice for studying the rubber elasticity of derived materials and assessed the molecular mechanisms of polymer physics.[2,3] Indeed, in addition to its chain flexibility and mobility, PDMS permits high control of network topology by end-linking reactions, vinyl-terminated polydimethylsiloxane with tetrakis(dimethylsiloxy)silane, for instance. Although the level of fundamental understanding is far from complete, the main concepts linking the material architecture to the mechanical properties are well understood. The main parameters describing the network topology are the molar mass between cross-linking points (molar mass of the elastic chains), as well as the contents of (i) dangling chains (chain attached to the network only by one end); (ii) chains loops (chain with both ends meeting at the same junction), and (iii) chains entanglements (Scheme 1). Obviously, each parameter impacts the material properties. First, whatever the theoretical molecular model considered to predict the elastic behavior of polymer network (from affine to phantom limit models), it is well-known that the modulus strongly depends on the molar mass between knots M_c.[4,5] If the network consists on short chains, brittle material with high tensile strength but small elongation at break is obtained. On the contrary, long chain-based network gives low ultimate strength but high extensibility. The molar mass distribution has also an influence on the elastomeric properties of a network.[6,7]

Another important point in polymer physics concerns all the chains elastically inactive, such as loops, dangling chains, and free chains. These defects clearly decrease the elastic properties of networks due to the reduction in the amount of elastically active chains, otherwise leading to a viscous modulus increase. The basic idea, proposed by de Gennes,[8] is that linear chains are free to reptate. Damping then originates from the viscoelastic relaxation via reptative motion of the free chains.[9] End-linked networks containing unattached chains exhibit high damping at a certain frequency which is controlled by the size of the free chains and the mesh size.[9,10] On the other hand, branched chains or pendant chains must relax by a different, slower mechanism, with movements from the free end to the fixed one. Villar et al.[11] proved that the loss modulus depends significantly on the concentration and molar mass of the dangling chains present in a network. In pendant chains, the relaxation time increases exponentially with the number of entanglements, while it varies in a power fashion for linear molecules.[11]

It is important to note that long dangling chains can also participate to the elasticity of the network. Indeed, for PDMS chains above a critical molar mass M_c, lying between 21 0 and 33 000 gmol^{-1} according to different authors,[12] physical entanglements between silicone chains act as cross-linking points separated by about 12 000 g mol^{-1}.[13,14] Ultimately, it was shown that reacting PDMS (M_n = 28 000 g mol^{-1}) in a swollen state, in a view to minimize entanglements of the chains between cross-linking points, strongly enhanced the strain at break up to 3000%.[15] At high frequency stress, pendant chains behave as additional elastic chains because of these entanglements, which cannot relax in that range of time or frequency.[16]

Multimodal networks combine the high elongation of long chain unimodal network and the high stress at break of short chain unimodal material. For instance, bimodal networks have been proven to present enhanced tensile test results compared to unimodal networks, due to the ability of the shorter chains to sustain most of the applied stress, whereas the more flexible long chains provide ductility.[17] On the contrary, the improvement in fracture energy of precut bimodal networks over that of unimodal networks is much less pronounced and appears to be dictated by the average molar mass of the effective elastic strands in each network.[17] By increasing the cross-linker functionality, the extent of reaction at the gel point decreases,[18] whereas the maximum stress and rupture energy are improved.[19]

The number of elastic chains can be obtained from the storage modulus by DMA measurements, whereas the tangent of loss angle tanδ, defined as the ratio E'/E'' of the storage (E') and loss (E'') moduli, evaluates the dissipation of the deformation.[20] For unfilled material obtained from end-linking PDMS chains without any defect, Sullivan[21] showed that tan δ depends only on the cross-linking density. The higher the molar mass between cross-linking points, the higher the tan δ. Urayama[10] prepared irregular networks, i.e., defects containing network and showed that, either by increasing the monofunctional chains content or by applying an off-stoichiometric ratio, tan δ increases whereas E' decreases. The pendant chains display relaxation (E'' increase) at characteristic frequency which depends on the molar mass, highest frequencies corresponding to the faster relaxation process, i.e., the shortest chains. Frequency-insensitive tan δ network can be obtained with broad size distribution of pendant branched chains.

2.2. Mechanical Properties of Model Filled Materials. To counteract the inherent weakness of silicone, formulations are generally filled with silica, the surface of which creates strong interactions with the polymer backbone. Improvements in moduli and ultimate properties involve a hydrodynamic effect arising from the inclusion of rigid particles and an increase in the cross-linking density created by polymer−filler bonding. In the absence of polymer−filler interactions, only hydrodynamic reinforcement is expected.[22] Far from the ideal networks assuming an uniform chain length between cross-linking points, the presence of filler particles randomly distributed in the material, creates heterogeneity of polymer chain lengths due to polymer−filler interactions.[23] The types of interactions which are determined by polymer adsorption include different kinds of entanglement interactions[24] and polymer bridging between filler particles.[25] One effect of the filler is to increase the orientation and the extension of the chains provoking an increase of both stress and material modulus.[26] The silica loading[27] as well as the filler morphology[28] defined by the surface area,[25] the residual hydroxyl groups[29] and the distribution of functional group (vinyl for instance) on the filler surface[30] may also change the aggregation state and thus the mechanical properties of silicone elastomers.[31−34]

The compression set (CS) measures the material ability to maintain its elastic properties after prolonged thermal aging under compression, high value of CS implying that the material does not recover its initial height. Although slightly different from compression set (which is a normal stress relaxation), the shear stress relaxation has been extensively investigated

theoretically[35−37] and experimentally by rheology.[38,39] Experimental stress relaxation data have been found to follow the empirical Chasset−Thirion equation[40] of the power law form

$$G(t) = G_e\left(1 + \left(\frac{t}{\tau_e}\right)^{-m}\right) \quad (1)$$

where $G(t)$ is the stress relaxation modulus, G_e is the equilibrium modulus, and m and τ_e are material parameters. τ_e is a characteristic time, the parameter m is predicted to be proportional to the cross-linking density and to the dangling chains molar mass.[16,41] Ferry[20] suggested that the molecular mechanism responsible for this long-time relaxation process is the diffusion of dangling chain ends. Curro and co-workers[42,43] developed two successive theories on the basis of the reptation of branched polymer molecules in the presence of topological entanglements.

The material ultimate properties, elongation at break and tensile strength, are measured by tensile tests through stress−strain curves. The Mooney-Rivlin equation permits to follow the modulus evolution as a function of the elongation reciprocal (vide infra). Generally speaking, during the tensile tests, three stages are observed: a first part where the modulus drops off, called the Payne effect, then a constant modulus region and a ternary part corresponding to a modulus increase ("stress upturn"). Recently, the Payne effect has been qualitatively described by a model composed of a filler network formed either directly between filler particles or through elastomer domains. In the latter case, the adsorbed elastomer on silica surface is glassy near the filler surface, so that its modulus gradually decreases with the distance from the filler surface. In addition, polymer may be entrapped in filler aggregates in so-called "occluded rubber clusters", which behave mechanically as a unique filler particle and thus artificially increase the filler content. The Payne effect would then originate from the breakage and reformation of such filler networks and clusters. This model describes the influence of (i) the filler specific area, (ii) the silica content, (iii) the extent of silanol on the silica surface, and (vi) the temperature on the Payne effect amplitude.[52−54]

The phenomenon occurring in the medium region has been extensively studied through examination of the Mullins effect. The Mullins effect is a stress softening that invariably occurs in silica-filled silicone elastomer during the first deformation compared to the second and subsequent elongations. Various theories including bond ruptures, molecule slipping, filler-cluster rupture, chain disentanglement, chain retraction, network rearrangement, and composite microstructure formation have been proposed.[55] Clement et al.[56] highlighted the molecular mechanism of Mullins effect from successive stretching cycles at various temperatures and conclude that this effect corresponds to the detachment or slippage of chains having reached their limited extensibility on the filler surface. Similarly, the final modulus upturn arises from the limited chain extensibility between cross-linking points.[57,58] Just before breaking, those chains that withstand the large stress highly contribute to the elastic modulus. The characteristic upturn is especially observed for bimodal network and shifts to smaller elongations as the number of short chains increases.[59] Recently, birefringence measurement have suggested that the limited chains extensibility may not be the sole contributor toward the bimodal reinforcement.[60]

Tear mechanism has been studied under threshold conditions, i.e., at low rates of tearing, at high temperature, and under a swollen state (using xylene for PDMS).[61] In principle, upon deformation, all chains of unimodal network carry the same force. Fracture would occur by a catastrophic dissociation of backbone bonds at a very critical stress. When overloaded, chains break irreversibly and transmit the load to neighboring chains, so that the elastic energy of the broken chain is dissipated into heat. To strengthen a network, then, one requires to reduce the stress concentration or, stated alternatively, to increase the uniformity of force among network chains by implementing a high cross-linking density.[62] According to Lake and Thomas,[61,63] the fracture energy expressed as the energy to tear through a unit area for unfilled elastomer can be calculated from

$$G_c = KM^{1/2} \quad (2)$$

In this equation, M is the molar mass of the elastic strand that is to be ruptured and K is a prefactor calculated from the polymer chain properties. A recent work[17] showed that the best correlation between molecular mass and G_c is obtained by using the molar mass between cross-linking points, taking into account the entanglements. In addition to the polymer chain properties, the fracture energy G_c comes from viscous dissipation, strain-induced crystallization, and deviation of the tear path in reinforced materials.[64,65] Crystallization is not a pertinent factor in PDMS networks as the experiments are carried out far from the PDMS melting point (235K). For unfilled materials, a steady tearing on "trouser" piece is observed while the filled materials showed unstable tearing (stick−slip tearing), especially at higher tearing rates. This effect has been explained by the deviation of the tear path from the straight-ahead direction by curving around and stopping when it encounters a filler agglomerate, followed by a possible new tear which then tends to repeat the same process. The largest increase in tear strength occurred in going from 0 to 10 wt % silica, with smaller increases in tear strength resulting upon further increase in silica content.[66] Higher strength of sulfur-cured networks (polychloroprene, styrene-butadiene rubber, polybutadiene and ethylene-propylene copolymer) compared to the same material cross-linked by peroxides was explained by the reversibility of polysulfidic linkages that break and reform when overloaded (also called "non catastrophic energy dissipation").[67] Hydrogen bonds between silica surface and polymer backbone might play similar role of energy dissipation without failure. Tear resistance increases with the silica content and with the specific area (for unmodified precipitated silica surface).[28] Contrary to elongation at break and tensile strength, tear resistance (and compression set) can be improved by incorporating inactive fillers which do not create hydrogen bonds into silicone-silica blends.[68] Yanyo and Kelley[69,70] observed improvements for bimodal compared to unimodal network. Genesky et al.[17] showed that improvement due to unfilled bimodal or trimodal networks compared to unimodal networks is much less pronounced for tear resistance than for tensile test. Enhancement appeared to depend on the average molar mass of the effective elastic strands in each network. At a molecular level, it has been determined that siloxane bond rupture occurs via an ionic mechanism producing charged products that interact with the silica surface.[71]

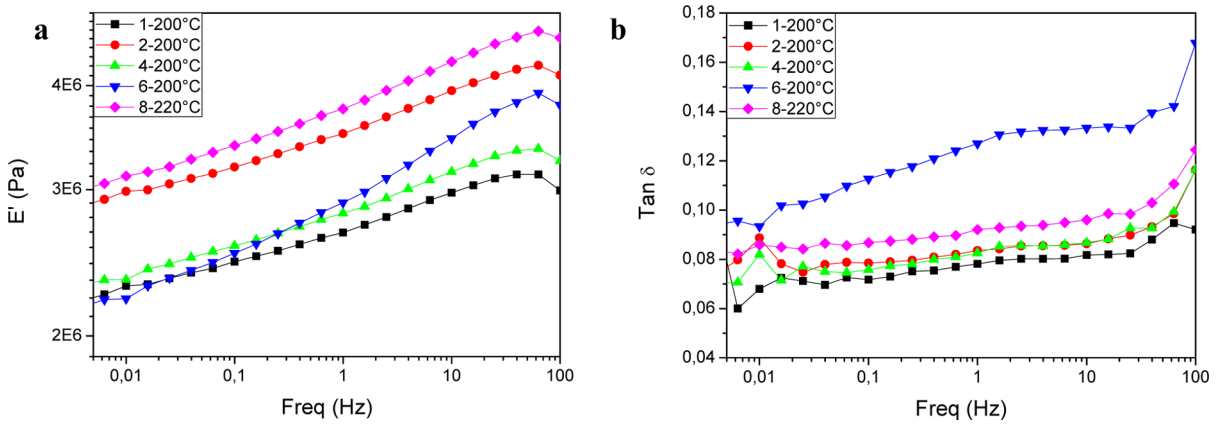

Figure 1. (a) Elastic modulus and (b) tan δ for 200 °C cured materials as a function of frequency.

3. EXPERIMENTAL SECTION

3.1. Materials. The silicone formulations were provided by different silicone suppliers. All the studied products are self-lubricating LSR grades for automotive applications, cured by injection molding machine at 180, 200, and 220 °C during 55, 47, and 36 s, respectively. Among the eight materials originally selected,[1] only 6 products presenting the same content of silica were chosen for studying their mechanical properties. Methylcyclohexane (ReagentPlus, 99% Sigma-Aldrich) and ammonia (puriss., anhydrous, ≥99.9%) were purchased from Sigma Aldrich and used as received in swelling measurements.

3.2. Methods. Dynamic mechanical analysis measurements were performed on cylindrical disk (13 mm diameter, 6 mm thickness) in compression with a plate−plate geometry in the linear domain at 30 °C, static and dynamic forces set at −0.5 and 0.4 N respectively. The network elasticity (E') originates from the network backbone while the dissipativity of networks (E'') arises from the network defects, such as dangling chains. The tangent of loss angle ($\tan \delta = E'/E''$) represents the proportion of dissipated energy recorded from 100 to 5×10^{-3} Hz (vide infra).

Compression Set measurements were carried out according to ISO 815 procedure. A cylindrical disk (13 mm diameter, 6 mm thickness) was compressed to 25% of its original height, using spacers to accurately set the strain. After 2 h at room temperature, the compression device was placed in an oven at 150 °C for 72 h. The sample was then removed from the oven, cooled for 30 min before measuring the final thickness. The compression set is expressed as the percentage of the original strain that is not recovered (eq 3).

$$CS = \frac{H_0 - H_f}{H_0 - H_c} * 100 \quad (3)$$

where H_0, H_f, and H_c are the initial, final and compressed height, respectively. All presented values are mean values from 5 experiments.

Tensile and tear tests were carried out as nonequilibrium, dynamic stress−strain measurements using a Zwick Proline Z005 tensile testing machine. Tensile and tear tests followed ISO 37 (type 2) and ISO 34 (method B without precut) norms respectively (see TOC graph showing the shapes of "dog-bone" and "right angle" specimens, used respectively). The sample was first placed between clamps initially separated by a distance of 50 mm; after a preloading step (0.5 N at 100 mm/min), the test specimen was lengthened at 500 mm/min until failure. At that speed, the sample is out of equilibrium. For comparison, Yoo[72] extended the samples at 20 mm/min, the maximum strain rate was selected after verifying that the stress−strain data were independent of strain rate. Five specimens of each material were tested.

Elongation is defined as the ratio $\Delta L/L_0$ (%), and modulus or "reduced stress" as

$$\text{modulus} = \frac{f}{A(\alpha - \alpha^{-2})} \quad (4)$$

where α is L/L_0; f and A^* represent the stress and the original undeformed cross section area, respectively. From stress−strain curves, values for the stress at break (i.e., tensile strength) and elongation at break were derived.

The tear strength Ts is calculated from

$$T_S = \frac{F}{d} \quad (5)$$

where F is the maximum force (N) and d the sample thickness (mm). For all experiments, five stress−strain curves were collected for each material.

4. RESULTS

4.1. Dynamic Mechanical Analysis Measurements. Figure 1a shows that except for material **6**, all the materials present similar behaviors as a function of frequency. The highest storage modulus on all the frequency range is observed for material **8**, followed by material **2**. The elastic modulus of material **6** at low frequency is due to long elastic chains, present in low content. It thus rapidly increases with frequency to solicit the short elastic chains, here in larger quantities; such atypical behavior points out the broad size distribution of elastic chains compared to other materials. Regarding the loss tangent, materials **1**, **2**, **4**, and **8** behave the same. The low tan δ of material **1** reflects highly cross-linked domains. Despite its high storage modulus, material **8** dissipates more energy because of the relaxation of the plasticizer introduced into the network. Again, material **6** presents atypical behavior with a marked increase of tan δ with frequency, suggesting a broad distribution of pendant chains.[73]

Studying the curing temperature effect on the network, tanδ evolution confirms the main trends already observed (Figure 2). For material **2**, high curing temperature strongly decreases the tangent of loss angle meaning that the amount of defects decreases. In agreement with the curing behavior, we show here the lack of reactivity of material **2** at 180 °C, contrary to material **4** that possesses the same cross-linking density and dangling chains amount when cured at 180 or 200 °C. Material **6** presented higher tan δ as the curing temperature increased. Two explanations are proposed here: either the curing reaction at 200 °C took place too rapidly, producing network defects such as dangling chains, or high temperature favored side reactions, such as radical addition of vinyl groups on methyl instead of hydride groups.

4.2. Compression Set Measurements. Compression set measures the height recovering of cylindrical disk after prolonged thermal aging under compression. Few studies

dx.doi.org/10.1021/am300503j | ACS Appl. Mater. Interfaces 2012, 4, 3353−3363

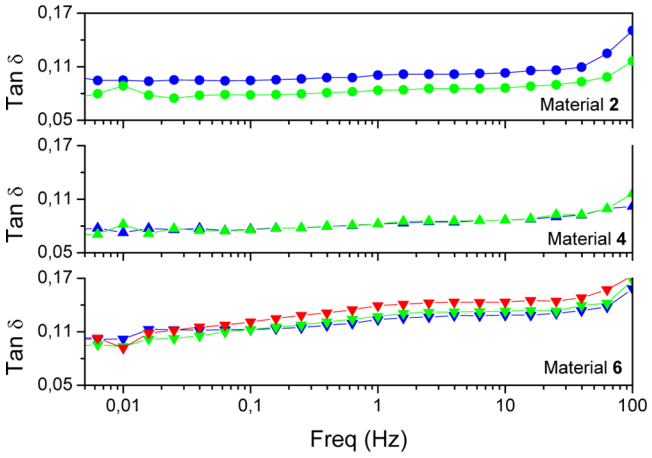

Figure 2. Tangent of loss angle as a function of curing temperature (180 °C, blue; 200 °C, green; and 220 °C red) for materials **2** (circle); **4** (up triangle) and **6** (down triangle).

exploring the compression set behavior of silicones are available in the open literature (see part 2.2), whereas some data are barely found in the patent literature. For instance, Fitzgerald et al.[44] claimed that the control of the surface silanol density in silica filler enables to control the percentage of the sealing force retention; in other words, by keeping the initial height (low compression set value), the sample maintains the "sealing" stress. Other patents report examples of adding small contents of high value specific additives to improve the compression set of the materials. Typically, the compression set is reduced when materials contain transition metals, for instance iron and tungsten sulfides, cadmium selenide[45] or iron−manganese spinel.[46] Another possibility described in some patents is to incorporate low contents of sulfur[47] and nitrogen compounds, such as quaternary ammonium[48,49] or ammonium carboxylate.[50] All these compounds increase the cross-linking density, especially through weak interactions. Working on the network topology, incorporation of vinylated resin ($MM^{Vi}Q$ or $M^{Vi}DQ$) has been proven to greatly enhance thermal aging properties.[51]

Cured at 200 °C, materials **1** and **4** present better compression resistances than material **2**; the worst results were observed for materials **6** and **8** (Figure 3). Except **2** and **8**, all materials vulcanized at 180 °C or at 200 °C present the same

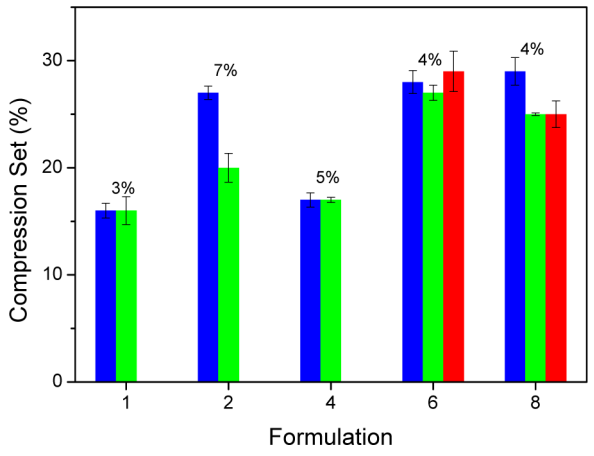

Figure 3. Compression set value after 72 h at 150 °C for materials cured at 180 °C (blue columns), 200 °C (green columns), and 220 °C (red columns). (Labels give the exuding oil's content).

CS value, in accordance with the fact that the cross-linking reaction is completed at a temperature as low as 180 °C (see part I of this series).[1] Increasing the curing temperature T_c significantly improved the material **2** compression set value, which is in agreement with the previous conclusions: 180 °C is not sufficient to fully cross-link the material (increasing T_c leads to higher elastic torque and lower tan δ).

Initially, the lubricant added in the formulations (see contents given in the labels Figure 3) was thought to play a significant role in the compression set value by freeing space inside the polymer matrix. Surprisingly, although this parameter must have his share in the unrecovered strain, other parameters seem to more significantly impact the CS value. For instance, the compression set values strongly correlate with the initial tangent of loss angle (Figure 4). Poor CS values were obtained

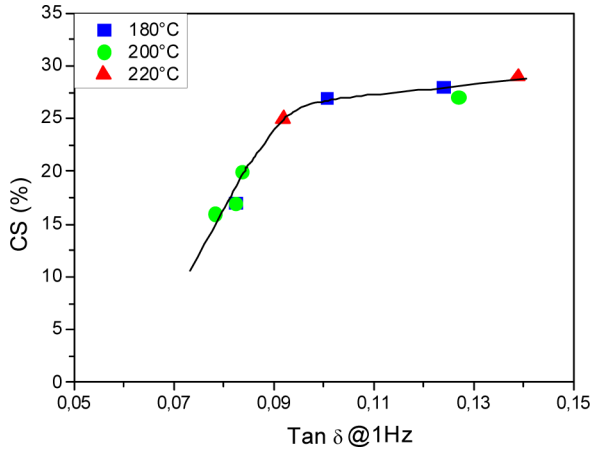

Figure 4. Influence of the tangent of loss angle (measured at 1 Hz) of different materials on its properties during the CS. Materials cured at 180 °C (blue squares), 200 °C (green circles), and 220 °C (red triangles). Line is only a guide for the eye.

for high tan δ values, which indicate an increase in the network ability to dissipate energy through network defects, for instance dangling chains, unconnected chains or polymer loops. These free-moving structures are able to dissipate the compressive stress by molecular motion and thus easily reorganize into the polymer network during the thermal aging.

According to the chemical analyses, the materials **1**, **2**, and **4** possess molar masses between cross-links far above the critical molar mass at which trapped entanglements are created, whereas material **6** stands on the breaking point and material **8** does not contain such structures (M_c^{Theo}, Table 1). Yilgor et al.[74] have proved that trapped entanglements permit a better recovery after elongation experiments. This behavior may explain (at least in part) the large compression sets observed for materials **6** and **8**. During the compression set experiment, the chemical structures can also change. For materials **1**, **2**, and **4** cured at 200 °C, the molar mass between cross-linking points, determined by swelling measurements before and after CS, remains constant (variations below 5%, see Figure 5a). On the contrary, post cross-linking occurred for the materials **6** and **8** as well as for material **2** when cured at low temperature. Formulation **6** contains a peroxide that cures the material at temperature as low as 140 °C, since all functional vinyl and hydride groups are consumed during the curing (see part I for details); if this peroxide is not totally consumed during the curing, the cross-linking reaction may be reactivated by the

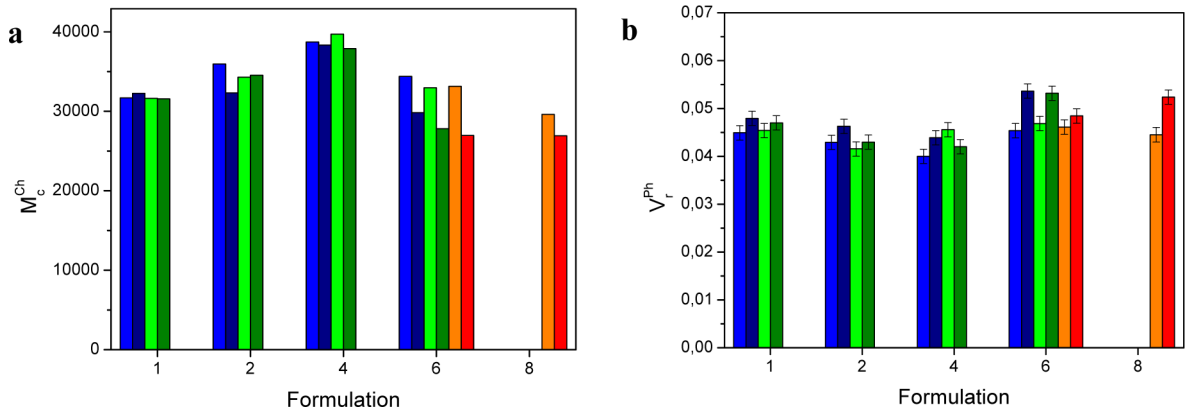

Figure 5. (a) Evolution of the molar mass between cross-linking points and (b) variation in the physical cross-linking extent during the compression set experiment (72 h at 150 °C) for materials cured at 180 °C (blue columns), 200 °C (green columns), and 220 °C (red columns); light and dark colors indicate the values taken before and after compression, respectively.

temperature increase during the CS experiment so as to connect methyl groups through radical coupling.[75,76]

For all materials, swelling measurements also allow to quantify the extent of hydrogen bonding increase during the thermal aging (for procedure details, see part I of this series)[1] (Figure 5b). For materials cured at high temperature, smaller evolution of hydrogen bond density was observed, most of the interaction being already created during processing (see Table S1 in the Supporting Information). Another interesting point is the dependence of CS on the initial hydride excess measured by ^{1}H NMR on un-cross-linked formulations (Figure 6). As no

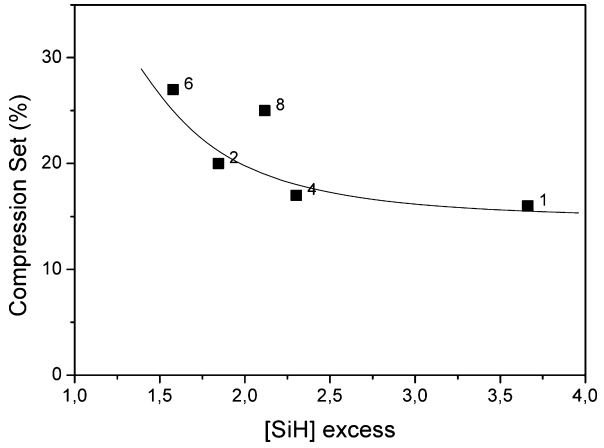

Figure 6. Influence of hydride excess on the CS value for materials cured at 200 °C (labels indicate the material name). Line is only a guide for the eye.

functional groups were observed after the curing process,[1] we concluded that SiH groups have reacted one with another to bridge the cross-linker molecules via short siloxane bonds instead of with long polydimethylsiloxane chains. A bimodal network is then created that is able to efficiently restrict molecular motion of free chains.[59] Mono or nonfunctional chains[1] induce higher compression set for formulation **8** than predicted by the trend detected in Figure 6.

In conclusion, during the CS tests, PDMS chains rearrange and filler−polymer interactions freeze the new configuration for all formulations, unless trapped entanglements or amount of hydrogen bonds created between silanols from the silica surface and polymer backbone during curing are sufficient enough to restrict the molecular motion. Very short chains that were generated during the curing by consuming the hydride excess also decrease the molecular rearrangement. Similarly, peroxide-cured formulation undergoes cross-linking reaction under compression and at high temperature. Besides, the network defects, such as highly mobile chains that easily rearrange, strongly impact the compression set value. Improving the CS value goes through reducing the chains mobility either by creating short chains (building a bimodal network through hydride excess) or by curing the material at higher temperature in the first place, i.e., increasing the extent of physical cross-linking.

4.3. Tensile tests. For most materials, strain−stress curves present an initial large drop in modulus while increasing elongation, followed by a more or less marked increase of modulus (Figure 7). Stress upturn occurs at high elongation for materials **1**, **2**, **4**, and **8**, the latter being particularly marked because of the high content of short elastic chains (Figure 7a), whereas for materials **6** and **7**, Figure 7b exhibits stress increase at low elongation followed by nearly linear variation of modulus, corroborating the broader distribution of elastic network strands.

Regarding the ultimate properties, material **7** (50 Shore A) provides the highest values of tensile strength with the lowest elongation at rupture (e.g., 4.9 MPa and 335%, respectively, for the material cured at 180 °C). Softer materials present similar tensile strengths while the elongation at break ranges from 550 to 700%. Concerning the tensile strength (Figure 8), best results are obtained for materials containing vinylmethylsiloxane units inside polymer chain (**2** and **8**, 0.16 and 0.85 D^{Vi} units per chain in average, respectively). The latter is slightly better thanks to higher stress upturn. Peroxide-cured materials **6** and **7** present the lowest results compared to the materials containing D^{Vi} units. Plotting the elongation at break E_b as a function of the molar mass between cross-linking points, measured by swelling, shows an interesting trend (Figure 8). Better agreement is found by plotting the molar mass between cross-linking points taking into account the chemical and physical cross-linking points than the sole chemical cross-linking density M_c^{Ch} (see part I for details on various parameters' measurements).[1] This result indicates that (at least part of) the hydrogen bonds are strong enough to behave as real cross-linking points. In agreement with Mark and Tang results on bimodal networks,[19] the elongation at break increases

dx.doi.org/10.1021/am300503j | ACS Appl. Mater. Interfaces 2012, 4, 3353−3363

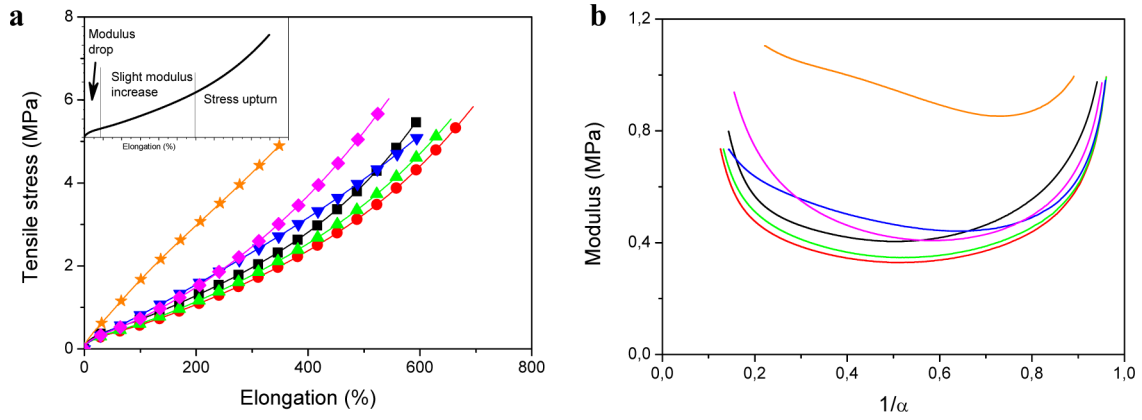

Figure 7. (a) Stress–strain curves and (b) Mooney–Rivlin plots for material **1** (black squares); **2** (red circles); **4** (green up triangles); **6** (blue down triangles); **7** (orange stars); and material **8** (purple diamonds) cured at 200 °C (see experimental section for calculation details).

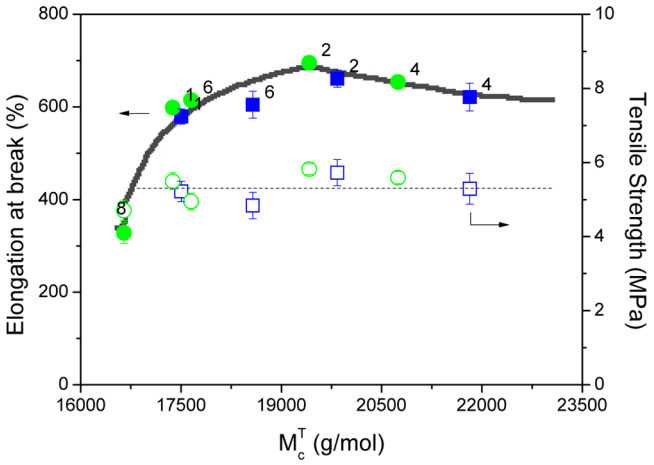

Figure 8. Elongation at break (solid symbols) and tensile strength (open symbols) for materials cured at 180 °C (blue squares) and at 200 °C (green circles). Lines are only guides for the eye.

with M_c, ranging from 660 to about 3000 g mol^{-1}. Here, although tensile strengths do not depend on M_c^T, optimum E_b is found for a M_c^T of 20 000 g mol^{-1}; increasing M_c^T above that point leads to a weakening of the material because of the too low cross-linking density. One should note that this optimum value stands near the critical value of molar mass between cross-links M_c at which trapped entanglements, separated by about 12 000 g·mol^{-1}, are generated. Yilgor and co-workers, while studying filled and unfilled thermoplastic PDMS-urea copolymers, likely showed that increasing the molar mass of soft segments, i.e., the molar mass between two physical cross-linking points, so as to overpass the critical molar mass at which entanglements are formed, led to an increase of the tensile strength, particularly in the absence of silica.[77,78]

4.4. Tear Resistance of LSR. For some of our materials, the tear did not appear clearly as a material rupture on the strain–stress curves (as an example, see Figure 9). Indeed, at 190 mm, we observed either a complete tear (**2**-b and **2**-e) or only a small stress decrease (**2**-a, **2**-c and **2**-d). In that case, the elongation to get complete tearing was at least doubled. We attributed this tear path deviation to the high loading level of silica (about 30% of silica particles for all materials), the tear being additionally deflected by strength-oriented chains. In these cases, the first stress decrease was taken as the force required to initiate the tear.

All the materials show tear strengths in the same range, except material **6** (Figure 10a). Surprisingly, the 50 Shore A material (**7**) was found only slightly better (T_s = 15.8 N/mm) than most of the 30 Shore A materials (tear strength between 12 and 14 N/mm). We did not find any clear correlations between tear strength and molar masses between chemical or physical knots, neither with the square root of M_c^T. For the

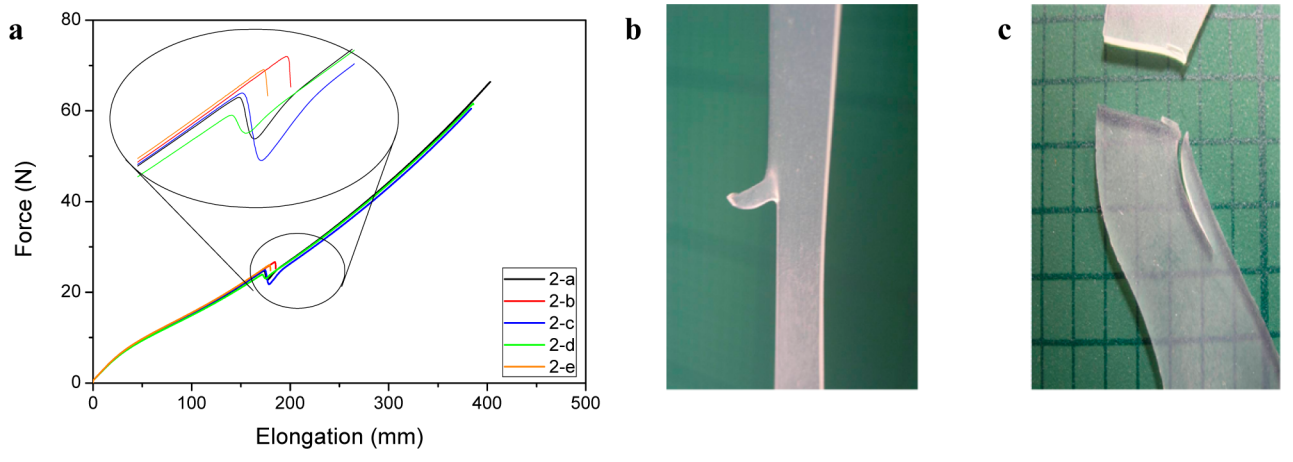

Figure 9. (a) Strain–stress curves reproduced 5 times of material **2** cured at 200 °C. Pictures taken (b) during and (c) after the tearing experiment.

dx.doi.org/10.1021/am300503j | ACS Appl. Mater. Interfaces 2012, 4, 3353–3363

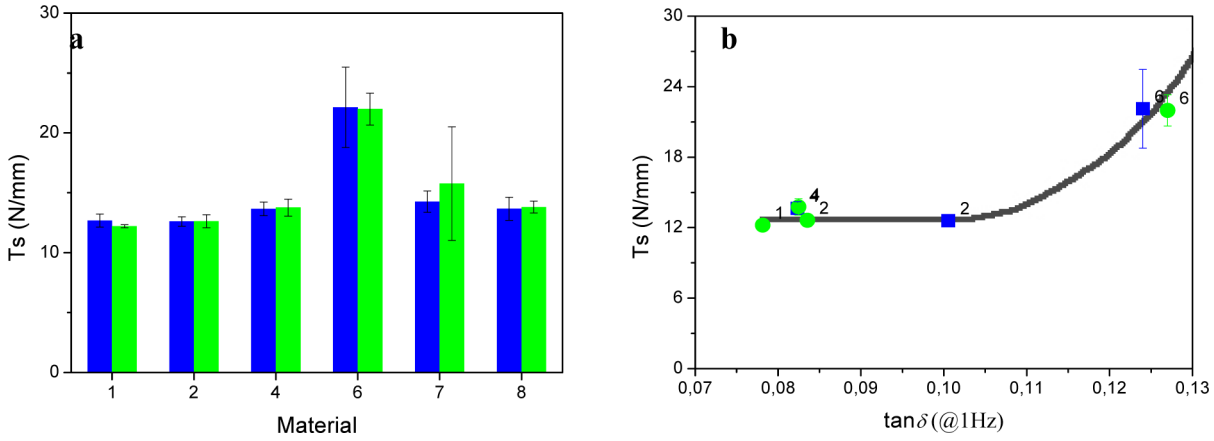

Figure 10. (a) Tear strength for materials cure at 180 °C (blue columns) and 200 °C (green columns); (b) correlation between T_S and tan δ, obtained from DMA (line is only a guide for the eye).

material **6**, however, the high tearing strength can be ascribed to the broad molar mass distribution between cross-linking points that has been also evidenced during the tensile test. Besides, that material highly dissipates mechanical energy as proved by DMA measurements (high tan δ, see Figure 10b). Such viscous dissipation might also explain the strong resistance of material **6** (Figure 8). The partially cross-linked material **2** (cured at 180 °C) exhibits an intermediate tan δ value that is not sufficient to improve the tear resistance.

5. DISCUSSION

Taking the whole picture of the chemical analyses and mechanical properties results, the main parameters governing the mechanical properties are the molar masses between cross-linking points (either through physical or chemical bonds) and their weight distribution, the contents of inelastic chains and the polymer−filler interactions.

Concerning the first point, elongation at break increases with M_c until reaching an optimum value around 20 000 g mol^{-1}, which roughly corresponds to the critical molar mass at which trapped entanglements are created. Tensile and tear strengths seem to greatly depend on the polydispersity of network strands. One should remark that, keeping constant the molar mass of the vinyl terminated PDMS, the cross-linker structure determines the polydispersity of the elastic strands through the number and the repartition of hydride functions into the cross-linker chain. Short chains act as single cross-linker of functionality f (Figure 11a), whereas for long cross-linker chains and/or low concentration of hydride groups compared to dimethylsiloxane units, the cross-linking point behaves as multiple cross-linking points with an average functionality of 3 (Figure 11b). Moreover, in that case, the oligomeric chains between two cross-linking points behave as small elastic strands engendering bimodal network. Similarly, the hydride conversion during the cross-linking reaction may change the cross-linker functionality.[5]

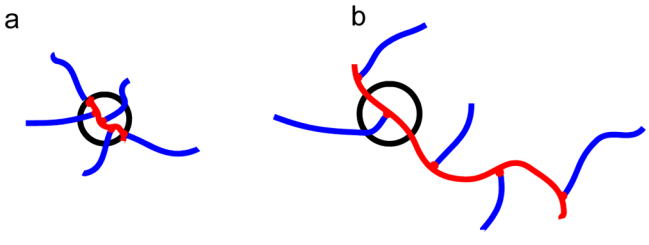

Figure 11. Structure and functionality of (a) short cross-linker, f = 5; (b) long and/or having few hydride groups (f = 3). Red and blue lines stands for the cross-linker and vinyl terminated PDMS chain, respectively; Black circles schematically represent the cross-linking point.

Thus, small excess of hydride groups and short cross-linker provide unimodal network in which all the cross-linking points are precisely separated by the molar mass of the vinyl terminated polymer. For such a network, no upturn is discernible.[79,80] Materials **6** and **7** seem to correspond to this type of strongly unimodal network, since the chemical analysis pointed out that they include in their formulation the shortest cross-linker (2400 g mol^{-1} against from 5000 to 7700 g mol^{-1} for materials **1**, **2**, and **4**) and the smallest ratio SiH/SiVi (around 1.4) compared to other materials. It is not excluded however that radical reactions randomly cross-link the PDMS chains, producing large size distribution of network chains as proved by the constant increase of modulus with elongation.

The influence of the second parameter, i.e., the content of inelastic chains, is better reflected while comparing the common LSR material, cross-linked by hydrosilylation, and the material obtained by peroxide catalysis. The network of the former presents more or less marked bimodal character because of hydride functions excess or incorporation of D^{Vi} unit into the chains, whereas the architecture of the latter is less controlled and thus possesses a very large distribution of molar mass between cross-linking points. As shown already, for the first network type, better control on vulcanization through hydrosilylation produces less free-moving structures that strongly impact the CS value and improves the tensile strength. Alternatively, peroxide-cured materials show enhanced tear strength thanks to broad chain size distribution networks, possibly assisted by a high dissipation factor. The compression set value is on the other hand degraded, compared to the first category, since post cross-linking reaction takes place during the experiment (probably because of continuation of radical reaction) and pendent chains rearrange on the silica surface.

The third parameter concerns the physical interactions with silica that play a great role for tensile test and tear resistance. Here, all the contributions, namely chemical knots and physical interactions, have to be taken into account. The latter, though weaker, plays a great positive role on these properties. Note

dx.doi.org/10.1021/am300503j | ACS Appl. Mater. Interfaces 2012, 4, 3353−3363

that if the physical cross-linking points do not go to completion during the curing process, the interactions between silica surface and polymer grow up during the thermal aging, leading to poorer results for compression set. Surprisingly, functionalization of silica surface with coupling agents such as vinyl groups (materials **2** and **7**) has not been found a critical parameter for enhancing the mechanical properties studied here; only a slight improvement in tensile strength could be attributed to the attachment of polymer matrix on the filler surface.

6. CONCLUSIONS

In this series of papers, eight commercial formulations were chemically characterized under un-cross-linked form and cured by injection-molding at 180 and 200 °C. The network topologies of these materials were primarily investigated by swelling measurements and confirmed by dynamic mechanical analysis. After curing, liquid silicone rubbers present elastomeric mechanical properties, namely elongations at break as high as 700%, tensile strengths around 6 MPa, compression set values from 15 to 25% after 72 h at 150 °C and tear strength from 12 to 21 N/mm. Around these mean values, the eight materials studied here present slight discrepancies of mechanical properties that have been ascribed to network topology variations. If the decrease in the content of dangling chains enhances the compression set value, in the same time, the tear resistance becomes worse. Molar mass between knots is maybe the most crucial parameter governing all the mechanical properties. In addition to the hardness, tensile test is also dependent on M_c; in the range studied here, we found that an optimal value exists providing the best elongation at break. Last but not least, the M_c distribution provides an outstanding contribution to mechanical properties such as compression set and tear strength. However, if a large distribution enhances the compression set and slightly improves the tensile strength through stress upturn, narrower distribution gives exceptional tear strength results. Against all expectations, a priori important parameters such as curing temperature and vinyl functinalization of silica surface only produced slight variation on the investigated properties and have been proved to be of less important for the materials studied here. Recently, Multi-Quantum Nuclear Magnetic Resonance (MQ-NMR) has been proved to be a powerful tool to probe the distribution of elastic strands in a cross-linked material.[81−83] This nondestructive and noninvasive method could open new outlook in the study of imperfect PDMS networks.[84]

■ ASSOCIATED CONTENT

Ⓢ Supporting Information

A table summarizing the main features of network structure. This material is available free of charge via the Internet at http://pubs.acs.org/.

■ AUTHOR INFORMATION

Corresponding Author

*Address: Ingénierie des Matériaux Polymères, UMR CNRS 5223, Bâtiment Jules Verne, 17, avenue Jean Capelle, 69621 Villeurbanne, France. Tel: 33 4 72 43 71 04. E-mail: francois.ganachaud@insa-lyon.fr.

Notes

The authors declare no competing financial interest.

■ ACKNOWLEDGMENTS

The authors acknowledge Pr. J-P Habas, Dr. A-S Caro, and Pr. L. Chazeau for fruitful discussions.

■ REFERENCES

(1) Delebecq, E.; Ganachaud, F. *ACS Appl. Mater. Interfaces* **2012**, DOI: 10.1021/am300502r.
(2) Erman, B.; Mark, J. E. *Compr. Anal. Chem.* **2008**, *53*, 337−383.
(3) Rubinstein, M.; Panyukov, S. *Macromolecules* **2002**, *35*, 6670−6686.
(4) Patel, S. K.; Malone, S.; Cohen, C.; Gillmor, J. R.; Colby, R. H. *Macromolecules* **1992**, *25*, 5241−51.
(5) Sharaf, M. A.; Mark, J. E.; Ahmed, E. *Colloid Polym. Sci.* **1994**, *272*, 504−15.
(6) Falender, J. R.; Yeh, G. S. Y.; Mark, J. E. *Macromolecules* **1979**, *12*, 1207−9.
(7) Falender, J. R.; Yeh, G. S. Y.; Mark, J. E. *J. Am. Chem. Soc.* **1979**, *101*, 7353−6.
(8) De Gennes, P. G. *Scaling Concepts in Polymer Physics*; Cornell University Press: London, 1979.
(9) Urayama, K.; Kawamura, T.; Kohjiya, S. *Polymer* **2009**, *50*, 347−356.
(10) Urayama, K.; Miki, T.; Takigawa, T.; Kohjiya, S. *Chem. Mater.* **2004**, *16*, 173−178.
(11) Villar, M. A.; Valles, E. M. *Macromolecules* **1996**, *29*, 4081−9.
(12) *Polymer Data Handbook*; Oxford University Press: New York, 1999.
(13) Acosta, R. H.; Monti, G. A.; Villar, M. A.; Valles, E. M.; Vega, D. A. *Macromolecules* **2009**, *42*, 4674−4680.
(14) Fetters, L. J.; Lohse, D. J.; Milner, S. T.; Graessley, W. W. *Macromolecules* **1999**, *32*, 6847−6851.
(15) Urayama, K.; Kohjiya, S. *Eur. Phys. J. B* **1998**, *2*, 75−78.
(16) Roth, L. E.; Vega, D. A.; Valles, E. M.; Villar, M. A. *Polymer* **2004**, *45*, 5923−5931.
(17) Genesky, G. D.; Cohen, C. *Polymer* **2010**, *51*, 4152−4159.
(18) Braun, J. L.; Mark, J. E.; Eichinger, B. E. *Macromolecules* **2002**, *35*, 5273−5282.
(19) Tang, M. Y.; Mark, J. E. *Macromolecules* **1984**, *17*, 2616−2619.
(20) Ferry, J. D. *Viscoelastic Properties of Polymers*, 3rd ed.; Wiley: New York, 1980.
(21) Sullivan, J. L.; Mark, J. E.; Hampton, P. G.; Cohen, R. E. *J. Chem. Phys.* **1978**, *68*, 2010−2012.
(22) Bokobza, L. *Macromol. Mater. Eng.* **2004**, *289*, 607−621.
(23) Hanson, D. E. *Polymer* **2004**, *45*, 1055−1062.
(24) Aranguren, M. I.; Mora, E.; Macosko, C. W. *J. Colloid Interface Sci.* **1997**, *195*, 329−337.
(25) Cochrane, H.; Lin, C. S. *Rubber Chem. Technol.* **1993**, *66*, 48−60.
(26) Yuan, Q. W.; Mark, J. E. *Macromol. Chem. Phys.* **1999**, *200*, 206−220.
(27) Zhang, C.; Liu, L.; Zhang, Z.; Pal, K.; Kim, J. K. *J. Macromol. Sci., Part B: Phys.* **2011**, *50*, 1144−1153.
(28) Cochrane, H.; Lin, C. S. *Rubber World* **1985**, *192*, 29−36.
(29) Osaheni, J. A.; Truby, K. E.; Silvi, N. *Macromol. Symp.* **2001**, *169*, 261−268.
(30) Maxson, M. T.; Lee, C. L. *Rubber Chem. Technol.* **1982**, *55*, 233−44.
(31) Demir, M. M.; Menceloglu, Y. Z.; Erman, B. *Macromol. Chem. Phys.* **2006**, *207*, 1515−1524.
(32) Aranguren, M. I.; Mora, E.; Macosko, C. W. *J. Colloid Interface Sci.* **1997**, *195*, 329−337.
(33) Boyle, J.; Manas-Zloczower, I.; Feke, D. L. *Part. Part. Syst. Charact.* **2004**, *21*, 205−212.
(34) In the commercial formulations studied here, attempts to isolate the filler failed because of the high compatibility between silica and PDMS. We anticipate that the materials are filled with comparable silica, i.e., modified through the in situ silazane grafting process.
(35) Heinrich, G.; Vilgis, T. A. *Macromolecules* **1992**, *25*, 404−7.

(36) Heinrich, G.; Havranek, A. *Prog. Colloid Polym. Sci.* **1988**, *78*, 59−62.
(37) Havranek, A.; Heinrich, G. *Acta Polym.* **1988**, *39*, 563−7.
(38) Batra, A.; Cohen, C.; Archer, L. *Macromolecules* **2005**, *38*, 7174−7180.
(39) Dickie, R. A.; Ferry, J. D. *J. Phys. Chem.* **1966**, *70*, 2594−2600.
(40) Chasset, R.; Thirion, P. *Phys. Non-Cryst. Solids, Proc. Int. Conf.* **1965**, 345−59.
(41) Vega, D. A.; Villar, M. A.; Alessandrini, J. L.; Valles, E. M. *Macromolecules* **2001**, *34*, 4591−4596.
(42) Curro, J. G.; Pincus, P. *Macromolecules* **1983**, *16*, 559−62.
(43) Curro, J. G.; Pearson, D. S.; Helfand, E. *Macromolecules* **1985**, *18*, 1157−62.
(44) Fitzgerald, J. J.; Osaheni, J. A.; Buddle, S. T.; Pero, D. T. *Heat-Curable Silicone Rubber Compositions with their Properties Controlled by the Density of Surface Silanol Groups on Fumed or Pyrogenic Silica Fillers*. U.S. 5 623 028, 1997.
(45) Steinberger, H.; Pesch, K. D.; Naumann, T. *Silicone Elastomers with Reduced Compression Set and Process for Preparing Them*. U.S. 5 219 922, EP 455 078, 1991.
(46) Johnson, T. D. *Silicone Rubber Having Reduced Compression Set*. U.S. 5 260 364, 1993.
(47) Kammerer, J.; Kovar, I.; Matejcek, K.-M.; Bosch, E.; Strassberger, W. *Liquid Compositions for Manufacture of Silicone Rubber Moldings with Improved Compression Set*. U.S. 5 977 249, 1998.
(48) Burkus, F. S., II; Jeram, E. M.; Rubinsztajn, S. *Curable Silicone Elastomers Having Low Compression Set*. U.S. 5 998 516, EP 926 208, 1999.
(49) Burkus, F. S., I. I.; Jeram, E. M.; Rubinsztajn, S. *Reduction of Compression Set of Liquid Injection Moldable Silicone Elastomers and Nitrogen Salts for Property Modification*. U.S. 5 977 220, EP 926 190, 1999.
(50) Osaheni, J. A.; Evans, E. R.; Doin, J. E. *Additive and Method for Enhancing the Heat Age Properties of Elastomers*. U.S.6 239 202, EP 1 048 693, 2000.
(51) Ward, B. J.; Jeram, E. M.; Striker, R. A. *Fast-Curing Silicone Compositions for Rubbers with Heat-Aging Resistance and Low Compression Set*. U.S. 5 863 969, EP 552 919, 1993.
(52) Wang, M.-J. *Rubber Chem. Technol.* **1998**, *71*, 520−589.
(53) Clement, F.; Bokobza, L.; Monnerie, L. *Rubber Chem. Technol.* **2005**, *78*, 232−244.
(54) Clement, F.; Bokobza, L.; Monnerie, L. *Rubber Chem. Technol.* **2005**, *78*, 211−231.
(55) Diani, J.; Fayolle, B.; Gilormini, P. *Eur. Polym. J.* **2009**, *45*, 601−612.
(56) Clement, F.; Bokobza, L.; Monnerie, L. *Rubber Chem. Technol.* **2001**, *74*, 847−870.
(57) Mark, J. E. *J. Inorg. Organomet. Polym.* **1994**, *4*, 31−44.
(58) Pan, S. J.; Mark, J. E. *Polym. Bull.* **1982**, *7*, 553−559.
(59) Kilian, H. G. *Colloid Polym. Sci.* **1981**, *259*, 1151−1160.
(60) Viers, B. D.; Mark, J. E. *J. Inorg. Organomet. Polym. Mater.* **2007**, *17*, 283−288.
(61) Gent, A. N.; Tobias, R. H. *J. Polym. Sci., Polym. Phys. Ed.* **1982**, *20*, 2051−8.
(62) Hamed, G. R. *Rubber Chem. Technol.* **1991**, *64*, 493−500.
(63) Lake, G. J.; Thomas, A. G. *Proc. R. Soc. London, Ser. A* **1967**, *300*, 108−19.
(64) Bhowmick, A. K. *J. Macromol. Sci., Rev. Macromol. Chem. Phys.* **1988**, *C28*, 339−69.
(65) Lake, G. J. *Rubber Chem. Technol.* **1995**, *68*, 435−60.
(66) Kumudinie, C.; Mark, J. E. *Mater. Sci. Eng., C* **2000**, *C11*, 61−66.
(67) Bhowmick, A. K.; Gent, A. N.; Pulford, C. T. R. *Rubber Chem. Technol.* **1983**, *56*, 226−32.
(68) Simon, M. W.; Stafford, K. T.; Ou, D. L. *J. Inorg. Organomet. Polym. Mater.* **2008**, *18*, 364−373.
(69) Yanyo, L. C.; Kelley, F. N. *Rubber Chem. Technol.* **1987**, *60*, 78−88.
(70) Yanyo, L. C.; Kelley, F. N. *Rubber Chem. Technol.* **1988**, *61*, 100−18.
(71) Lupton, E. M.; Achenbach, F.; Weis, J.; Braeuchle, C.; Frank, I. *ChemPhysChem* **2009**, *10*, 119−123.
(72) Yoo, S. H.; Yee, L.; Cohen, C. *Polymer* **2010**, *51*, 1608−1613.
(73) Bejenariu, A. G.; Boll, M.; Lotz, M. R.; Vraa, C.; Skov, A. L. *Proc. SPIE* **2011**, *7976*, 79762V/1−79762V/8.
(74) Yilgor, I.; Eynur, T.; Bilgin, S.; Yilgor, E.; Wilkes, G. L. *Polymer* **2011**, *52*, 266−274.
(75) Baquey, G.; Moine, L.; Degueil-Castaing, M.; Lartigue, J. C.; Maillard, B. *Macromolecules* **2005**, *38*, 9571−9583.
(76) Baquey, G.; Moine, L.; Babot, O.; Degueil, M.; Maillard, B. *Polymer* **2005**, *46*, 6283−6292.
(77) Yilgor, E.; Eynur, T.; Kosak, C.; Bilgin, S.; Yilgor, I.; Malay, O.; Menceloglu, Y.; Wilkes, G. L. *Polymer* **2011**, *52*, 4189−4198.
(78) Yilgor, I.; Eynur, T.; Yilgor, E.; Wilkes, G. L. *Polymer* **2009**, *50*, 4432−4437.
(79) Llorente, M. A.; Andrady, A. L.; Mark, J. E. *Colloid Polym. Sci.* **1981**, *259*, 1056−61.
(80) Llorente, M. A.; Mark, J. E. *Macromolecules* **1980**, *13*, 681−5.
(81) Saalwaechter, K.; Gottlieb, M.; Liu, R.; Oppermann, W. *Macromolecules* **2007**, *40*, 1555−1561.
(82) Maxwell, R. S.; Chinn, S. C.; Solyom, D.; Cohenour, R. *Macromolecules* **2005**, *38*, 7026−7032.
(83) Mayer, B. P.; Lewicki, J. P.; Weisgraber, T. H.; Small, W.; Chinn, S. C.; Maxwell, R. S. *Macromolecules* **2011**, *44*, 8106−8115.
(84) It is worth mentioning that the curing process significantly changes the mechanical properties. We prepared samples by compression method which consists on filling cold plate shaped mold and curing at 180 °C at 150 bar during 10 min. Such materials showed similar elongation at break but lower tensile strength (except **4**). Also, by preventing chains orientation parallel to the filling flux as observed in injection molding, many fewer tear deviations were observed and higher tear strength was measured.